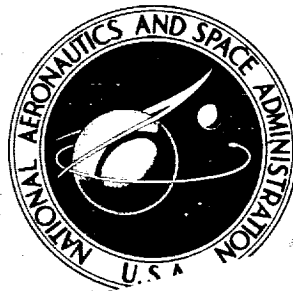


# NASA TECHNICAL REPORT



NASA TR R-264

NASA TR R-264

GPO PRICE \$ \_\_\_\_\_  
 CFSTI PRICE(S) \$ 3.80  
 Hard copy (HC) \_\_\_\_\_  
 Microfiche (MF) 0.65  
 # 853 July 65

**N 67 - 90127**  
 (ACCESSION NUMBER) \_\_\_\_\_ (THRU) \_\_\_\_\_  
29 -405 1  
 (PAGES) (CODE)  
 (NASA CR OR TMX OR AD NUMBER) \_\_\_\_\_ (CATEGORY) 01

## REVIEW OF PROPELLER-ROTOR WHIRL FLUTTER

*by Wilmer H. Reed III*

*Langley Research Center*

*Langley Station, Hampton, Va.*

[The page contains extremely faint and illegible text, likely bleed-through from the reverse side of the document. The text is mostly horizontal lines and fragments of words that cannot be transcribed.]

136



**REVIEW OF PROPELLER-ROTOR WHIRL FLUTTER**

By Wilmer H. Reed III

Langley Research Center  
Langley Station, Hampton, Va.

**NATIONAL AERONAUTICS AND SPACE ADMINISTRATION**

---

For sale by the Clearinghouse for Federal Scientific and Technical Information  
Springfield, Virginia 22151 - CFSTI price \$3.00



## REVIEW OF PROPELLER-ROTOR WHIRL FLUTTER

By Wilmer H. Reed III  
Langley Research Center

### SUMMARY

A survey is made of the state of the art of propeller-whirl flutter – a precession-type instability that can occur on a flexibly mounted aircraft engine-propeller combination. This report reviews the literature relating to this problem from the time it first became of concern on conventional turboprop and V/STOL aircraft.

Included in the survey are a description of the basic mechanism of whirl flutter, a summary of generalized trend studies on idealized systems, the status of methods for predicting propeller aerodynamic coefficients, the effects of flapping hinged blades and twisted flexible blades on whirl flutter, and some approaches for including propeller whirl modes as a part of the flutter evaluation for complete aircraft. Also, brief consideration is given to the response of flexibly mounted propeller-nacelle systems to random atmospheric turbulence.

Whirl flutter of conventional propeller-nacelle systems is now a reasonably well understood phenomenon and amenable to analysis. For propeller-rotor systems with flapping blades, however, comparisons between experiment and theory suggest the need for further refinements in the mathematical model.

### INTRODUCTION

Although the phenomenon known as propeller-whirl flutter – a dynamic instability that can occur in a flexibly mounted aircraft engine-propeller combination – was discovered analytically by Taylor and Browne (ref. 1) in 1938, it was not until its "rediscovery" in 1960 that it was identified as a problem of practical concern.

Following the loss of two turboprop aircraft it was established in wind-tunnel investigations (ref. 2) at NASA Langley Research Center that propeller-whirl flutter could have occurred if the nacelle stiffness was severely reduced, for example, by a structural failure. In the undamaged condition the aircraft had an adequate margin of safety from whirl flutter. In addition to this wind-tunnel investigation for a specific configuration, some generalized trend studies were also conducted at Langley Research Center in order to identify and study the basic parameters involved in propeller-whirl flutter. (See refs. 3 to 6.)

As a result of these experiences on a turboprop aircraft, and the fact that VTOL configurations are likely to have unconventional propeller-rotor systems, whirl flutter has now become a design consideration on new propeller-driven aircraft. These considerations are reflected in recent amendments to U.S. Civil Air Regulations (ref. 7) which require that whirl flutter be included as a part of the dynamic evaluation of transport aircraft, and that no flutter shall occur as a result of failure of any single element of an engine mount structure.

The purpose of this report is to review work relating to propeller whirl flutter since the time the phenomenon became the subject of intensive investigation in 1960. The material presented herein essentially follows that given by the author in a recent review article (ref. 8) on the subject but with some additional background information included for completeness.

Following a description of the basic mechanism of propeller whirl flutter, the report summarizes some principal findings of generalized trend studies for idealized systems, next reviews the status of propeller aerodynamic coefficients used for the prediction of whirl flutter, and then illustrates how whirl stability of an idealized system can be altered by the use of propeller-rotors with hinged blades or highly flexible twisted blades. The next two sections deal with the question of incorporating propeller whirl modes into analytical and wind-tunnel flutter studies of the aircraft treated as a complete system. Finally, consideration is given to dynamic loads associated with the response of a flexibly mounted propeller-nacelle system to random atmospheric turbulence.

## SYMBOLS

a	distance between nacelle pivot point and plane of propeller in propeller radii
$C_T$	thrust coefficient, $\frac{\text{Thrust}}{\rho \left(\frac{\Omega}{2\pi}\right)^2 (2R)^4}$
$c_\theta, c_\psi$	nacelle viscous damping coefficients in pitch and yaw directions, respectively
$EI_2$	bending stiffness of cantilevered nacelle in pitch direction
e	hinge offset distance of flapping-blade propeller
$F + iG$	oscillating lift function

$H_{\theta,u}, H_{\theta,v}, H_{\theta,w}$	frequency response function giving response in $\theta$ to unit sinusoidal inputs in $u/V$ , $v/V$ , and $w/V$ , respectively
$h$	wing bending deflection
$I$	total moment of inertia of propeller-nacelle system about pivot
$I_x$	mass moment of inertia of propeller about rotation axis
$J$	advance ratio, $\frac{\pi V}{\Omega R}$
$K_{\theta}, K_{\psi}$	effective linear spring constants of cantilevered nacelle in pitch and yaw directions, respectively
$L_y, L_z$	total aerodynamic force due to propeller in $y$ and $z$ directions, respectively
$M_y, M_z$	total aerodynamic moment due to propeller about $y$ and $z$ axes, respectively
$R$	blade tip radius
$r$	radius of propeller blade section from rotational axis
$S_{\theta}, S_{\psi}$	torsional spring constant in pitch and yaw directions, respectively
$t$	time
$u, v, w$	components of gust velocity (see fig. 15)
$V$	forward flight speed
$x, y, z$	coordinate axes (see fig. 3)
$z_1$	natural mode shape of nacelle pitch mode
$\alpha$	angle of attack

$\alpha_1$	wing torsion angle
$\alpha_T$	inclination of thrust axis
$\zeta$	viscous damping of engine mount system relative to critical damping
$\theta$	pitch angle of propeller axis
$\theta_1$	inclination of propeller axis for unit deflection in natural pitch mode $z_1$
$\mu$	damping ratio of whirl mode (positive – unstable, negative – stable)
$\rho$	air density
$\Phi_u, \Phi_w, \Phi_\theta$	power spectra and cross spectra, where subscripts denote the associated time histories
$\psi$	yaw angle of propeller axis
$\Omega$	propeller rotational frequency
$\omega$	whirl frequency
$\omega_b$	cantilever fundamental frequency of nonrotating propeller blade
$\omega_h$	uncoupled wing bending frequency with rigidly attached nacelle and nonrotating propeller
$\omega_\theta, \omega_\psi$	fundamental natural frequencies in pitch and yaw, respectively, with nonrotating propeller
$\omega_1$	first coupled natural wing bending frequency

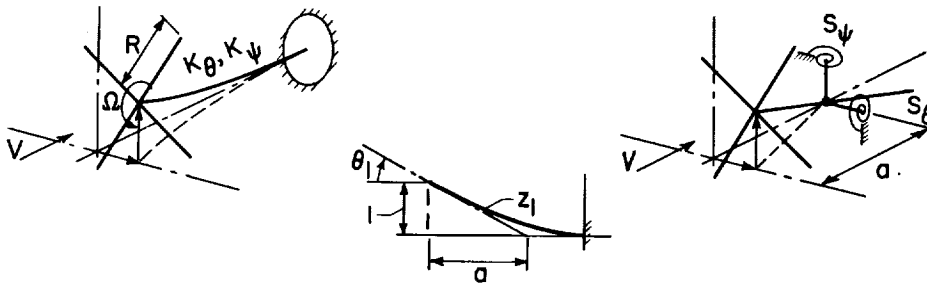
A dot over a symbol denotes differentiation with respect to time.



# MECHANISM OF PROPELLER WHIRL FLUTTER

## Idealized System

To introduce the basic ingredients of propeller whirl flutter, the idealized systems shown schematically in figure 1 will be used. On the left side of the figure the powerplant and nacelle structure are represented by a cantilever beam having continuous arbitrary distribution of mass and stiffness; on the right is shown an equivalent representation in which a rigid powerplant structure is assumed to be spring-restrained about a pivot located a distance  $a$  behind the propeller.



EQUIVALENCE:

$$\frac{1}{\theta_1} \quad \text{EQUIVALENT TO} \quad a$$

$$K_\theta = \int E I_2 z_1''^2 dx \quad \text{EQUIVALENT TO} \quad \frac{S_\theta}{a^2} \quad \text{ETC}$$

Figure 1.- Idealized propeller-nacelle systems (ref. 4).

When the cantilever system is approximated by a single pitch mode and a single yaw mode the two systems are exactly equivalent. For example, the cantilever system has an effective pivot distance  $a$  which is simply  $1/\theta_1$ , where  $\theta_1$  is the inclination of the propeller axis corresponding to a unit deflection in the natural pitch mode  $z_1$ . This and other equivalent relations between the two systems are established in reference 4.

The governing equations of motion for the idealized system may be derived from Lagrange's dynamic equation. (See ref. 4.) For the pivoted-powerplant system these equations are as follows:

Inertial terms  
Damping terms  
Elastic terms  
Gyroscopic terms  
Aerodynamic terms

Pitch:  $I\ddot{\theta} + c_{\theta}\dot{\theta} + S_{\theta}\theta - I_X\Omega\dot{\psi} = aL_Z + M_Y$

Yaw:  $I\ddot{\psi} + c_{\psi}\dot{\psi} + S_{\psi}\psi + I_X\Omega\dot{\theta} = aL_Y + M_Z$

The origin of the various forces and moments acting on the system are indicated above the equations. Note that in addition to the usual inertia, damping, and elastic forces, the spinning propeller introduces gyroscopic and aerodynamic forces. Since these latter two forces are distinguishing features of propeller whirl flutter they will be discussed in greater detail in the following subsections.

#### Role of Propeller Gyroscopic Forces

The influence of gyroscopic forces on the natural vibration modes of the idealized system can be illustrated with the aid of figure 2. When the propeller is not rotating, and aerodynamic and damping forces are neglected, natural vibrations of the system can occur independently about either the pitch axis or the yaw axis as shown by the left-hand side of figure 2.

When the propeller is rotating, however, the natural vibration modes cannot be excited independently, but are coupled by gyroscopic action of the spinning propeller. The natural modes of the system are then characterized by whirl or precession modes in reference to the manner in which the propeller hub whirls or precesses about the static thrust axis. These modes are so indicated by the center sketch in figure 2; again aerodynamic and damping forces have been neglected. Even for systems having symmetrical stiffness properties, the natural whirl frequencies would be different. The higher frequency mode is defined as the forward whirl mode and is associated with a whirl of the hub in the direction of propeller rotation. Similarly, the lower frequency mode is defined as the backward whirl mode and is associated with a whirl opposite to that of propeller rotation.

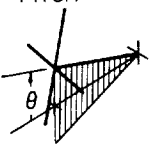
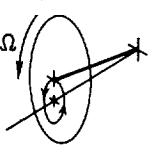
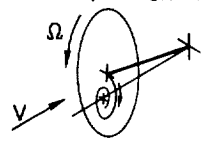
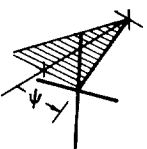
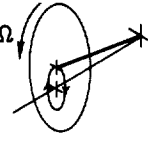
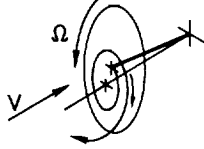
NATURAL VIBRATION MODES		
NONROTATING PROP.	ROTATING PROP. WITHOUT AIR FORCES	TRANSIENT RESPONSE WITH AIR FORCES
<p>PITCH</p> 	<p>FORWARD WHIRL</p> 	<p>STABLE (<math>V &lt; V_{CRIT}</math>)</p> 
<p>YAW</p> 	<p>BACKWARD WHIRL</p> 	<p>UNSTABLE (<math>V &gt; V_{CRIT}</math>)</p> 

Figure 2.- Natural vibration modes of system with rigid propeller.

### Role of Propeller Aerodynamic Forces

Since whirl modes produce angle-of-attack changes on blade elements of the propeller, aerodynamic forces are generated; these are the forces that provide the mechanism for instability. This instability for rigid-blade systems invariably occurs in the backward whirl mode. When the propeller blades have flap hinges or are very flexible, however, an instability in the forward mode is possible.

The sketches on the right-hand side of figure 2 give an example of the manner in which the system would respond in the backward whirl mode following a disturbance such as a gust. When the airstream velocity is less than the whirl flutter velocity  $V_{crit}$ , the path traced by the propeller hub is a spiral that converges to the original static equilibrium position. When the flutter speed is exceeded, however, a small disturbance will result in a diverging spiral motion of the hub which will continue to build up until the structure fails or its motion becomes limited by nonlinearities.

Some fundamental properties of the aerodynamics of a pitching and yawing propeller can be demonstrated, as in reference 9, by consideration of a propeller blade element. In figure 3 are shown the propeller force and moment vectors that can be significant. Drag forces on the blade element have been neglected. Also, the propeller thrust force is omitted from the figure because, as will be discussed later, thrust has only a small effect on whirl flutter. The vectors shown in figure 3 arise as a result of three distinct types of motions associated with a whirl mode: angular displacement of the propeller shaft in

pitch (or yaw), the rate of change of pitch (or yaw) angle, and lateral (or vertical) velocity of the shaft. Because of symmetry, only motions in one plane need be considered; the pitch plane is shown in figure 3. It should be noted, however, that interference effects of a nearby wing can result in unsymmetrical aerodynamic forces on the propeller.

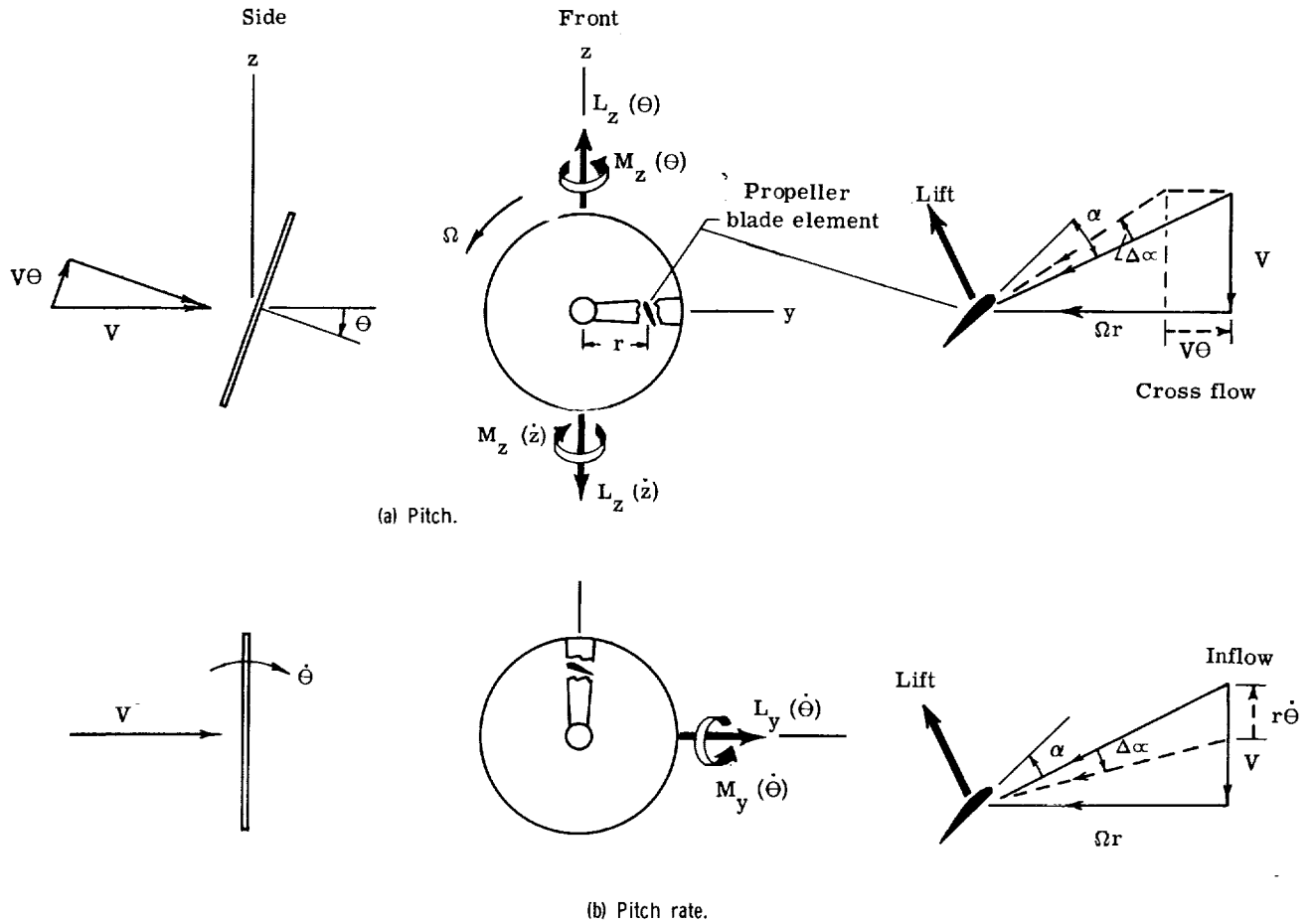


Figure 3.- Aerodynamic forces and moments on a pitching and plunging propeller at zero thrust.

When the propeller shaft is inclined at an angle  $\theta$  relative to the free stream, the forward velocity has a cross-flow component  $V_\theta$  in the plane of the propeller disk. With reference to the sketch of a blade element in figure 3(a), it can be seen that on the up-going side of the propeller disk this cross-flow velocity component tends to reduce both the relative velocity and the angle of attack of the blades; alternatively, blade elements on the down-going side of the propeller disk experience an increase in relative velocity and angle of attack. If the lift force on a blade element due to these angle-of-attack and velocity changes is resolved into components parallel and normal to the

propeller disk plane and these components then integrated over a cycle of propeller rotation, the net effect is a vertical force  $L_z(\theta)$  and a yaw moment  $M_z(\theta)$  having the directions indicated in figure 3(a). Note that the vertical force is in a direction to increase the pitch angle and therefore opposes the structural spring restoring force – a fact which makes possible the occurrence of a static divergence for very low levels of mount system stiffness.

The yawing moment due to pitch  $M_z(\theta)$  may be interpreted as a cross-stiffness term. This important term is the driving moment of propeller whirl flutter. Note that it produces a moment which is in the same direction as the yawing velocity for the backward whirl mode. Thus, this term acts as negative (destabilizing) aerodynamic damping which must be compensated by other positive damping forces if the system is to be stable. The aerodynamic part of the total damping available for this purpose may be found in the force  $L_z(\dot{z})$  and in the moment  $M_y(\dot{\theta})$  produced by the rate terms  $\dot{z}$  and  $\dot{\theta}$ , respectively. The damping force  $L_z(\dot{z})$  is equal and opposite to the vertical force due to pitch  $L_z(\theta)$ , but is associated with the effective angle  $\dot{z}/V$  ( $\dot{z} = a\dot{\theta}$  for pivoting system) rather than with the geometric angle  $\theta$ . During whirl the yawing moment  $M_z(\dot{z})$  associated with vertical velocity is in phase with the yaw angle and therefore acts as an aerodynamic stiffness term.

The damping due to pitch rate  $M_y(\dot{\theta})$  (fig. 3(b)) arises because of velocity components normal to the propeller disk. From the blade element diagram in figure 3(b) it can be seen that the inflow velocity due to pitch rate  $r\dot{\theta}$  results in an increased angle of attack on blade elements in the disk area above the horizontal pitch axis and a decreased angle of attack in regions below the pitch axis. The integrated effects produce a direct damping moment  $M_y(\dot{\theta})$  and a cross-damping force  $L_y(\dot{\theta})$ . This cross-damping force behaves as a stiffness term in the yaw plane in a manner similar to that of the cross-damping moment  $M_z(\dot{z})$ . Except for conditions near static divergence, the stiffnesses associated with these cross-damping terms, as well as the term  $L_z(\theta)$ , are small relative to the structural stiffness of the powerplant mount.

In summary, the propeller aerodynamic term important with regard to whirl flutter is the yaw moment due to pitch, or equivalently, the pitch moment due to yaw. This cross-stiffness moment drives the system in the backward whirl mode and is resisted by the aerodynamic and structural damping moments. At the critical whirl flutter speed, the energy input by the aerodynamic driving moment is exactly balanced by the energy absorbed by damping, such that oscillations of the system become self-sustaining (or neutrally stable).

# WHIRL FLUTTER CHARACTERISTICS OF TWO-DEGREE-OF-FREEDOM SYSTEMS

## Generalized Studies

The basic phenomenon of propeller whirl flutter for systems that comprise a rigid propeller and a flexibly mounted powerplant, such as that illustrated in figure 1, is now reasonably well understood. The stability characteristics of such systems have been investigated analytically over a rather broad range of parameters (refs. 3, 4, and 5). In addition, wind-tunnel studies have been conducted (ref. 6) to evaluate the theoretical prediction of propeller aerodynamic derivatives as well as whirl flutter stability boundaries.

A general finding of these studies is that whirl flutter is strongly dependent on such system parameters as stiffness, damping, pivot location, and propeller advance ratio. The influence of these and other parameters on whirl flutter stability boundaries for the two-degree-of-freedom system is briefly summarized in the following subsections.

### Stiffness and Speed Stability Boundaries

Some typical whirl flutter stability boundaries presented in reference 4 illustrate the combined effects of stiffness, flight speed, and propeller advance ratio for a particular system. The system used for illustration was two times stiffer in yaw than in pitch and had an effective pivot point located  $a/R = 0.585$  behind the propeller disk. Figure 4

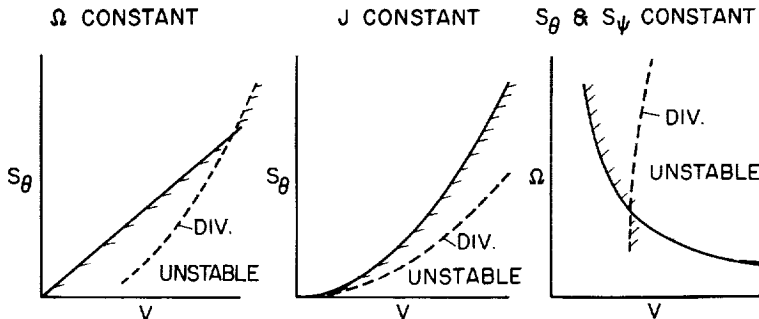


Figure 4.- Illustrative stiffness and speed boundaries (ref. 4).

shows the system stability boundaries for the following three cases of practical importance: constant propeller speed constant advance ratio, and constant stiffness.

#### Constant propeller speed.-

The first condition represents the usual constant-propeller-speed flight operation; the associated stiffness-airspeed stability boundary is shown on the

left side of figure 4. At the lower airspeeds the stiffness required to prevent whirl flutter is relatively low. As speed is increased larger stiffnesses are required for stability, and for sufficiently high speeds stability becomes governed by static divergence instead of flutter.

Constant advance ratio.- The condition for constant advance ratio, illustrated by the plot in the center of figure 4, corresponds to a windmilling propeller having a fixed blade angle. The use of windmilling propellers is a convenient wind-tunnel test procedure

and can be justified on the basis that propeller thrust generally has a small effect on whirl flutter. Again, these stability boundary plots depict the variation of stiffness required to prevent whirl flutter as a function of airspeed. In this case, however, the curves are parabolas – that is,  $S_{\theta}$  is proportional to  $V^2$  or, in other words,  $S_{\theta}$  varies linearly with dynamic pressure. Note that, in contrast to the previous case, divergence would not be encountered for this particular choice of system parameters.

Constant stiffness. - Finally, with stiffness held constant the stability boundaries involving propeller speed and forward speed are illustrated on the right side of figure 4. The unstable region is above and to the right. An important implication of the plot is that for operation on the nearly vertical portion of the curves a large change in propeller speed can occur without altering the critical speed appreciably, but that for operation on the nearly horizontal portion of the curve, the critical speed is quite sensitive to small changes in propeller speed; however, at these lower propeller speeds the instability is governed by static divergence rather than by whirl flutter.

#### Stiffness Ratio

Some additional typical whirl flutter trends are illustrated in figure 5. On the left side of the figure is plotted the critical pitch stiffness against the critical yaw stiffness for a given combination of forward speed, damping, and other system parameters. The stability boundaries are indicated by the shaded lines, and the lines radiating from the origin represent lines of constant stiffness ratio. Note in particular that the whirl flutter boundary is extended along the diagonal ray  $S_{\theta} = S_{\psi}$ ; this indicates that if a system had equal pitch and yaw stiffnesses it would be more prone to flutter than if one of the stiffnesses was appreciably reduced. The shape as well as the location of this curve, however, may be altered appreciably by the amount of structural damping in the system (see ref. 4). The lines that intersect each end of this boundary denote the stiffnesses required to prevent static divergence of the system.

#### Nacelle Damping

The center plot in figure 5 indicates the powerful stabilizing influence which mechanical damping usually has on whirl flutter. Because of this important influence, it is not feasible to neglect damping in whirl flutter analyses, as is frequently done in wing flutter analyses – to do so would in many cases result in a gross underestimation of the flutter speed. To predict whirl flutter in practical applications it is therefore desirable to obtain an accurate estimate of the powerplant-mount system damping. Damping measurement obtained during ground vibration test on an engine suspension system is discussed in reference 9. It is of interest to note that since the damping of the rubber engine mounts varied with temperature, a correction factor was determined by measuring

the damping characteristics of the mount at elevated temperatures in an environmental chamber.

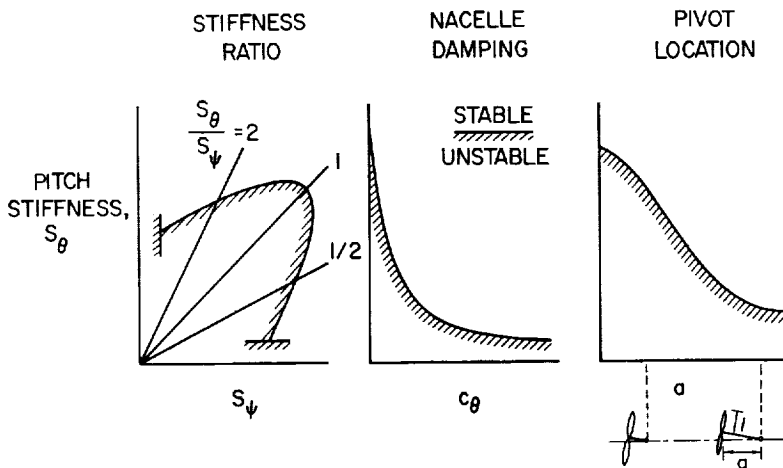


Figure 5.- Résumé of propeller-whirl trend studies.

### Pivot Location

The effect of location of the pivot axes on whirl stability is illustrated on the right side of figure 5. Note that moving the pivot location aft has a significant stabilizing influence. This fact, incidentally, can be attributed to the aerodynamic damping force associated with the transverse velocity of the propeller hub, that is,  $L_z(\dot{z})$  in the notation of figure 3. In addition to reducing the required stiffness,

moving the pivot aft tends to make the system less sensitive to changes in structural damping, because aerodynamic forces then become the predominant source of damping.

## PROPELLER AERODYNAMICS

As previously discussed, the pitching and yawing oscillations that accompany propeller-nacelle whirl motions produce aerodynamic forces on the propeller which in turn provide the driving mechanism for instability. Several methods are available for predicting the aerodynamic forces and moments required in a whirl flutter analysis. Ribner's analysis (ref. 10) of yawed propellers has long been used in studies of aircraft stability and is equally useful in propeller whirl flutter studies. (See, for example, ref. 3.) Houbolt's strip theory analysis (see ref. 4) lacks some of the refinements of Ribner's method, but is simpler to apply and appears to give comparable results. Both theories involve the assumption of quasi-steady aerodynamic forces and small angle-of-attack changes.

### Measured Derivatives

To evaluate theoretical methods for predicting propeller whirl flutter, an experimental investigation was conducted (ref. 6) in which both whirl flutter boundaries and propeller aerodynamic derivatives were measured. The wind-tunnel model, which resembled the previously described idealized mathematical model, consisted of a



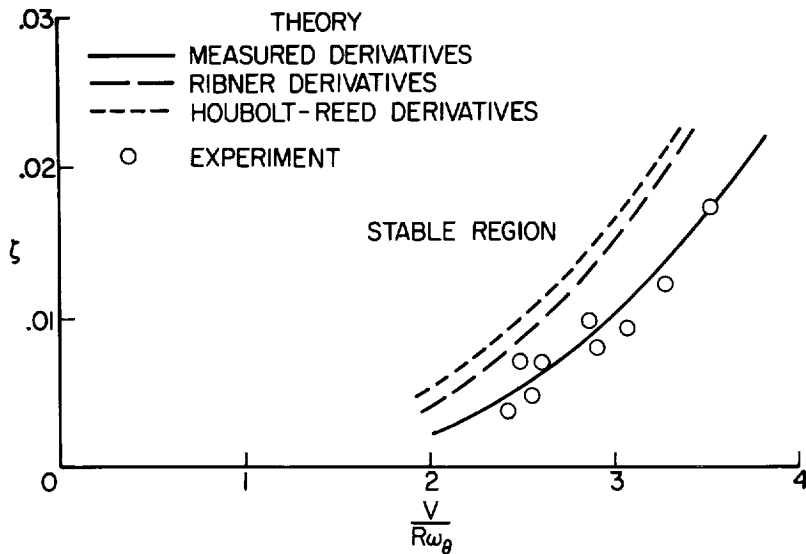


Figure 6.- Comparison of theoretical and experimental whirl-flutter boundaries for an axisymmetric system with rigid propeller (ref. 6).

windmilling propeller mounted on an isolated nacelle having symmetrical stiffness in pitch and yaw. Typical results from the study are presented in figure 6 which shows the nacelle damping ratio required to prevent flutter plotted against a nondimensional velocity. The calculated flutter boundaries were determined on the basis of three sets of aerodynamic derivatives: the theoretical derivatives derived by the methods of references 4 and 10, and the

actual derivatives as measured on the model. Note that the calculations based on measured derivatives are in excellent agreement with the experimental data, whereas those based on theoretical derivatives follow the same trends but tend to underestimate the observed flutter speed.

### Unsteady Flow

The differences in the flutter boundaries based on theoretical and measured derivatives may in part be due to unsteady aerodynamic effects. It can be shown that aerodynamic phase lags associated with the oscillatory wake have a stabilizing effect on the usual backward-mode whirl flutter. The theoretical derivatives used in figure 6 were modified to account for phase lags on the basis of the Theodorsen circulation function  $F + iG$  for two-dimensional airfoils. This approximation is good for very large advance ratios; however, for smaller advance ratios, the circulation function is significantly altered because of the helical pattern of the wake.

Studies (refs. 11 and 12) indicate that for low advance ratios the phase lag for a propeller can be much larger than would be predicted by the classical  $F + iG$  function for two-dimensional airfoils. It is interesting to note that for lowest advance ratios investigated in reference 6 ( $J = 1.3$ ) the measured phase lag was  $24^\circ$  as compared with a maximum possible theoretical value, based on Theodorsen's function, of  $13^\circ$ .

## Thrust

It has been established theoretically that propeller thrust has a relatively insignificant effect on whirl flutter stability for conventional rigid propellers under high-speed flight conditions. This fact greatly simplifies the construction and testing of wind-tunnel models in that it permits the use of windmilling rather than thrusting propellers. In a theoretical investigation of the effects of propeller thrust on whirl flutter (ref. 13), it is shown that thrust causes large deviations in the propeller derivatives at low-speed high-thrust flight states, such as take-off. However, at higher forward speeds where whirl flutter normally occurs, the deviation between aerodynamic coefficients for thrusting and windmilling propellers is usually less than 5 percent. Similar conclusions are found in reference 14 on the basis of experimental coefficients obtained on a thrusting propeller.

## High Inflow Angles

In the transition maneuver of VTOL aircraft from vertical to horizontal flight the inflow angle — that is, the angle between the thrust axis and the airstream  $\alpha_T$  — may be as large as  $90^\circ$ . At these high angles the propeller aerodynamic derivatives are likely to have values that differ

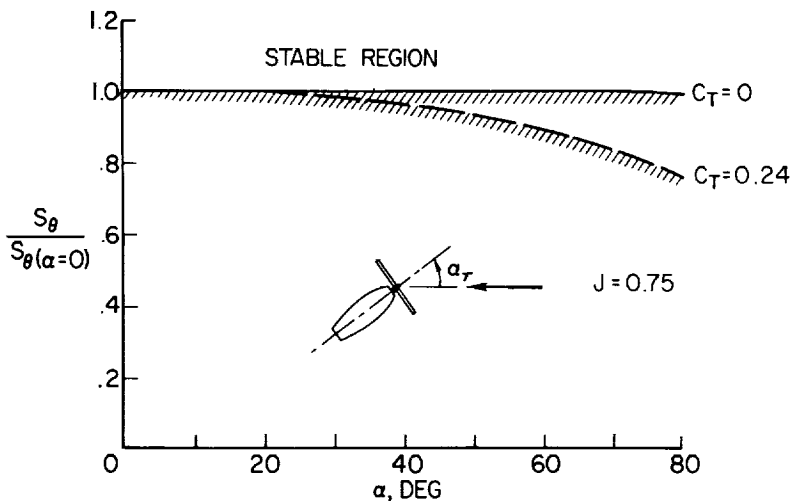


Figure 7.- Effect of inflow angle on stiffness required to prevent whirl flutter (ref. 14).

markedly from those corresponding to high-speed flight conditions. (See refs. 15 and 16.) Since whirl flutter is usually considered to be a relatively high-speed flight phenomenon it is of interest to explore the possibility of encountering whirl flutter in low-speed flight during transition. This question was briefly examined in reference 14. On the basis of whirl flutter calculations, which utilized experimental propeller derivatives and a simple axi-

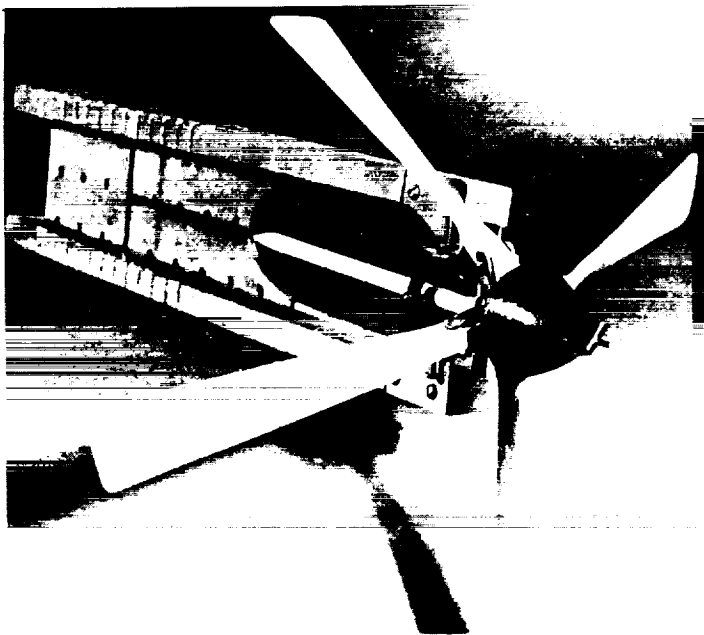
symmetric nacelle, angle-of-attack effects were found to be stabilizing in that the stiffness required to prevent flutter at high inflow angles was slightly less than that required at low angles. These results are summarized in figure 7 for a windmilling and a thrusting propeller.

## NONRIGID PROPELLER ROTORS

The generalized studies of classical propeller whirl flutter in references 3 to 6 were restricted to rigid propellers. This assumption is reasonable for conventional propeller-driven aircraft; however, V/STOL designs often incorporate articulated and flexible propeller-rotor systems that are compromises between the long flexible blades of a helicopter rotor and the short stiff blades of an aircraft propeller. It is therefore of interest to consider the manner in which whirl flutter might be altered by the use of nonrigid propeller-rotor systems. Of equal interest is the question of how rotor mechanical instability – an instability fed by energy of the rotating rotor rather than by the airstream – might be altered by the inclusion of aerodynamic forces associated with propeller whirl.

### Flapping Blades

Recent studies.– The effects of flapping hinged blades on whirl flutter have been examined in several recent studies. In a generalized study (ref. 17), a considerable number of parametric variations were investigated analytically and some complementary test data presented for a low-speed wind-tunnel model. An analysis of a whirl-flutter type of instability that was encountered on the XV-3 aircraft – a VTOL configuration with two-bladed see-saw propeller-rotor system – is presented in reference 18. This analysis



included, in addition to blade flapping, the effects of control coupling between the rotor and the pylon mounting structure.

The remainder of this section will concern a brief exploratory study of whirl flutter on the simple flapping blade model discussed in reference 14.

Wind-tunnel model.– The model, shown in figure 8, consisted of a windmilling propeller attached to a rod which has freedom to pitch and yaw about a set of gimbal axes. The system had symmetrical stiffness that could be controlled by varying tension in a spring connected axially at

Figure 8.- Flapping-blade propeller-whirl model investigated in reference 14. L-67-1008

the other end of the rod. Each propeller blade was attached to the hub by means of two pins, such that when both pins were in position the blades were fixed, and when one of the pins was removed the other pin became a flap hinge. In this way the blades could be hinged at either 8 or 13 percent of the propeller radius from the spin axis.

Experimental stability boundaries. - Whirl-flutter boundaries for the flapping-blade and fixed-blade conditions are presented in figure 9. During the test the model encountered both forward and backward whirl instabilities. The system became unstable in the backward mode for the fixed blade and the 13-percent hinge offset, but instability developed in the forward mode with the smaller hinge offset of 8 percent. Note that for flutter in the backward mode, blade flapping had a significant stabilizing influence; the opposite conclusion is indicated for flutter in the forward mode. In addition to the frequency differences, other changes in the system behavior were observed. Whereas backward whirl instability was accompanied by divergent motions as would be predicted by linear theory, forward whirl instability was characterized by amplitude-limited motions which could be excited when the disturbing force exceeded a threshold level.

Comparisons with theory. - Results of a theoretical analysis of the flapping-blade model are also shown in figure 9. This analysis, based on the method of reference 17 and considered further in reference 8, involves four degrees of freedom as follows: pitch and yaw of the propeller disk about the gimbal axis and cyclic flapping of the blades in the pitch and yaw directions normal to the propeller.

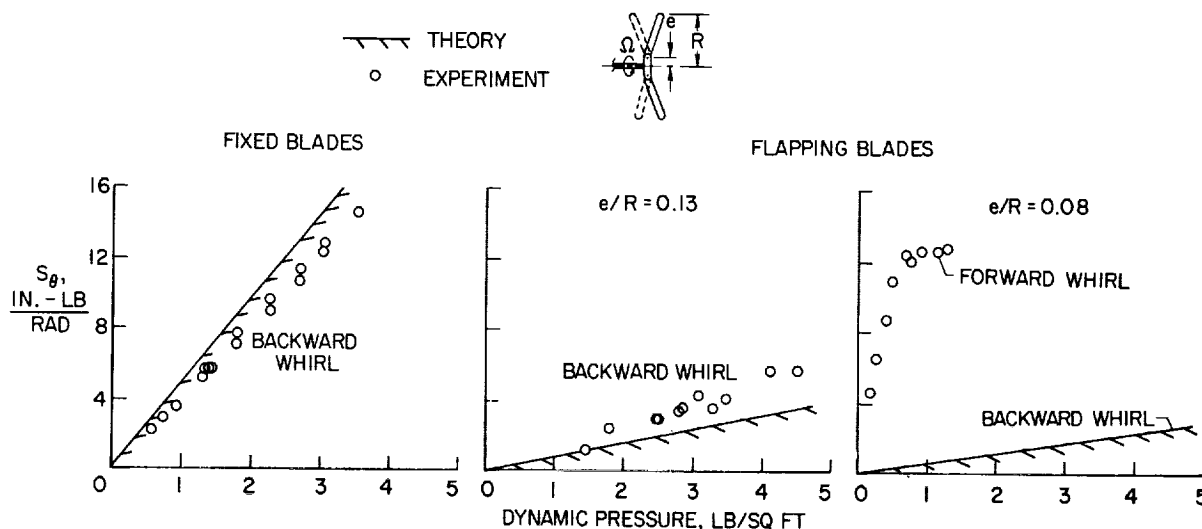


Figure 9.- Comparison of calculated and measured whirl-flutter boundaries for flapping-blade model investigated in reference 14.

From roots of the characteristic equation associated with these four degrees of freedom, the calculated frequency and damping of the flapping-blade whirl modes are as presented in figure 10 for the case of a 13-percent hinge offset. These roots are plotted against the ratio of propeller rotational frequency  $\Omega$  to the pitch frequency of the system with a nonrotating propeller. Since the propeller is windmilling,  $\Omega$  is proportional to

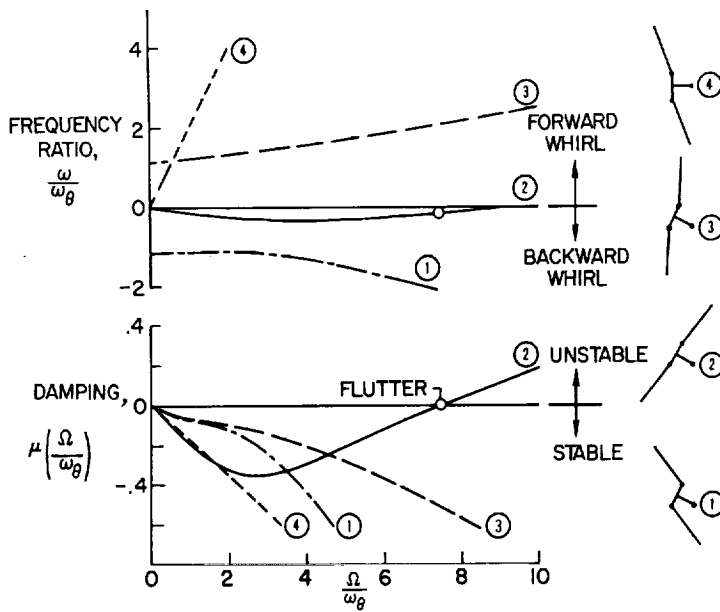


Figure 10.- Calculated flapping-blade whirl modes for  $e/R = 0.13$  (ref. 8).

the airstream velocity. Note from the plot of damping, that the stability of all but one of the modes increases continuously with increasing  $\Omega$ . The critical mode in this case (identified as ② in fig. 10) becomes neutrally stable when  $\Omega/\omega_\theta = 7.5$ . The whirl mode shapes calculated at the propeller frequency ratio corresponding to flutter are also indicated in figure 10. Note the relatively small contribution of blade flapping present in the unstable mode.

The theory and experiment shown in figure 9 are in reasonable agreement for the two cases where flutter occurred in the backward

whirl mode, that is, for the fixed blades and the flapping blades with a 13-percent hinge offset. However, the theory did not predict the forward whirl mode instability encountered with the 8-percent hinge offset. (See plot on right side of fig. 9.) It should be noted that in reference 17 a similar forward whirl mode instability was observed on a flapping-blade model which, again, theory did not predict. By modifying the theory in order to introduce an arbitrary phase lag in the propeller aerodynamic forces, a forward mode instability could be predicted; the required phase lag was  $30^\circ$ . For the configuration in figure 9, however, phase lags as high as  $45^\circ$  were assumed (see ref. 8), but the predicted instability always developed in the backward whirl mode. It therefore appears that this mathematical model lacks some of the ingredients needed to predict the whirl stability characteristics of flapping-blade systems.

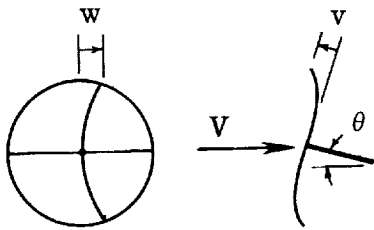
### Flexible Twisted Blades

General.- Bending deformations of a twisted propeller blade differ from those of the previously discussed flapping blade in a fundamental way. Whereas the flapping motion of a hinged blade was assumed to be normal to the propeller plane, the bending motion of a flexible blade with twist has components of displacement in the propeller plane as well as components normal to the plane. The relative contribution of these two components to a bending vibration mode of the blade will depend on such factors as its geometric pitch angle and the spanwise location of the root chord (i.e., the hub diameter).

The in-plane motions permitted by blade flexibility make possible the occurrence of another class of self-excited vibrations which, unlike propeller-whirl flutter, is purely mechanical in origin. This phenomenon, popularly called ground resonance, has received considerable attention in helicopter studies (e.g., refs. 19 and 20) and has also been recognized as a potential problem on tilt-wing V/STOL configurations (ref. 21).

A recent study of the interaction between propeller-whirl flutter and mechanical instabilities on systems having flexible twisted propellers is presented in reference 22. In this study, as in reference 17 for hinged propellers, a considerable number of parametric variations were analyzed theoretically and wind-tunnel tests were conducted on a simple low-speed wind-tunnel model.

The mathematical and physical models considered in this study consisted of an axisymmetrical nacelle and a flexible twisted propeller having a rigid hub and three or more uniform constant-chord blades. The relevant blade bending modes which can couple with whirl flutter are shown to be cyclic "pitch" and cyclic "yaw" motions in which the tip path plane is pitched or yawed because of blade bending. Each of these modes has associated with it an in-plane component of displacement. The flexible-blade mode illustrated in the following sketch is the pitch mode accompanied by in-plane bending. It is found that coning motions of the blades do not couple with the modes involved in the whirl instabilities and, consequently, this mode was not included in the analysis.



Mechanical instability in vacuo.- Some principal findings of the studies in reference 22 are presented in figures 11 and 12 of this report. Figure 11 shows the stability characteristics of one of the configurations analyzed for a condition of zero damping and without aerodynamic forces (e.g., as in a vacuum). There is close similarity between these plots and the Coleman frequency diagrams for mechanical instability (ref. 19). As the propeller rotational

speed  $\Omega$  increases, a point is reached where two of the frequencies coalesce, resulting in two modes at the same frequency, one of which is damped and the other unstable. This point, denoted by A in the figure, marks the beginning of a region of mechanical instability in a forward whirl mode.

Effects of air density.- Figure 12 shows the effects of adding aerodynamic forces to the stability analyses by progressively increasing air density from zero, the value assumed in figure 11. (Point A in fig. 11 lies on the zero density curve in fig. 12.) Stability boundaries are presented in figure 12 as plots of blade frequency against nacelle frequency for both forward and backward whirl modes. Boundaries for the forward mode originate from a mechanical instability; those for the backward mode originate from a whirl-flutter instability.

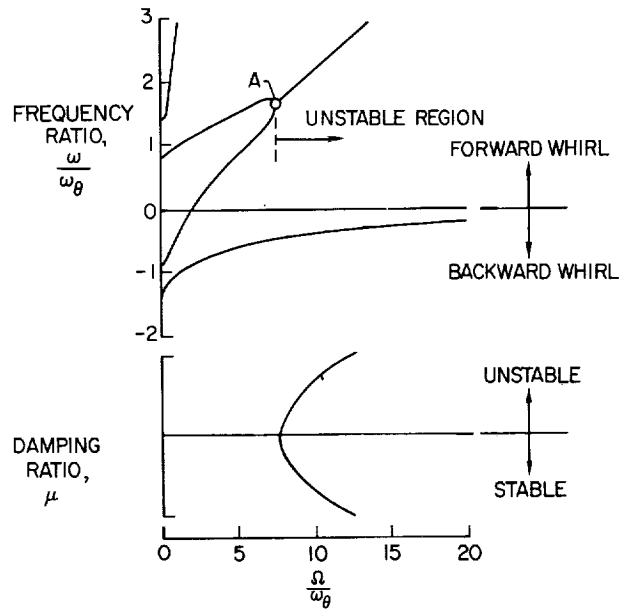


Figure 11.- Mechanical instability of system with flexible propeller in vacuo (ref. 22).

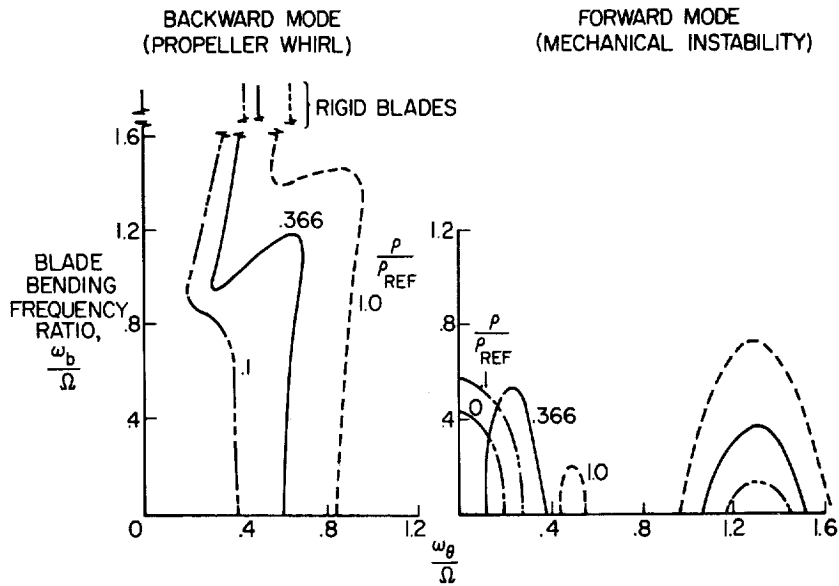


Figure 12.- Effect of air density on stability of system with a flexible-blade propeller (ref. 22).

Note (fig. 12) that in the forward whirl mode as air density increases two regions of instability develop. The region that has the higher values of  $\omega_\theta/\Omega$  is not of practical significance because the rate of growth of the unstable motions involved was found to be extremely low and would be eliminated by a small amount of structural damping. The other region of instability in the forward whirl mode is made worse initially as density increases, but with further increase in density the area of instability is reduced and eventually eliminated. It is interesting to note from this figure that the system encounters mechanical instabilities only if the nonrotating blade natural frequency  $\omega_b$  is less than the rotational frequency of the propeller.

With regard to propeller-whirl flutter — indicated by the stability boundaries for the backward mode — it appears that blade flexibility has relatively little effect except in a region where the blade frequency parameter  $\omega_b/\Omega$  is near unity. The asymptotic boundaries for a rigid propeller are also shown for comparison.

## REMARKS ON THE INCLUSION OF PROPELLER-WHIRL MODES IN WING FLUTTER ANALYSES

### General Considerations

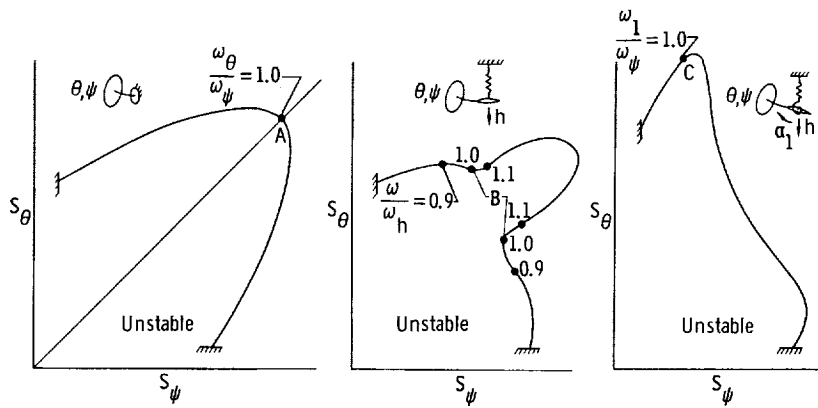
Although the idealized propeller-nacelle systems treated thus far in this report have been useful in explaining basic aspects of whirl flutter, more complex representations are usually required to evaluate the flutter characteristics of actual systems. Of particular interest is the effect of wing flexibility on whirl-flutter stability, and conversely, the effect of propeller-whirl modes on flutter stability of the wing. The purpose of this section will be to first discuss some general trend studies relating to the effects of wing flexibility on whirl flutter and then to review briefly some cases wherein whirl modes have been incorporated into the flutter clearance analysis for specific aircraft.

### An Analog Trend Study

It has been found that when a propeller-nacelle system is mounted on a flexible wing the whirl-flutter speed is generally higher than if the system were mounted on a rigid back-up structure. The wing in this instance tends to act as a damped-mass oscillator, capable of absorbing energy from the whirl mode. This observation may not apply, however, in cases where the wing flutter speed with rigidly attached nacelles is close to the whirl-flutter speed of the isolated propeller-nacelle system.

This tendency for the aerodynamic forces on a flexible wing to stabilize whirl flutter has been demonstrated in an analog computer study (ref. 23). Typical results from that study are presented in figure 13 for three cases: (a) a rigid wing, (b) a wing having freedom to translate vertically, and (c) a wing having freedom to translate and rotate





(a) Rigid wing. (b) Wing bending mode. (c) Wing bending torsion mode.

Figure 13.- Influence of wing flexibility on whirl flutter (adapted from ref. 23).

about an elastic axis. In the latter two cases, aerodynamic forces are assumed to act on the wing as well as on the propeller.

Consider first the case of a rigid wing. Features of this stability boundary are typical of those found in reference 4 and discussed previously with reference to figure 5. Again, it is to be noted that the boundary is extended along the diagonal ray  $S_\theta = S_\psi$  such that the symmetrical system, indicated by point A in figure 13(a), is the most critical from the standpoint of whirl flutter. The points at which this curve terminates are the static divergence boundaries for the system.

When the wing has freedom to oscillate in vertical translation (fig. 13(b)) it can be seen that its effect on whirl flutter is always stabilizing. This increased stability can be attributed to aerodynamic damping forces on the wing. It is of particular interest to note the "neck-down" portion of the curve where the stabilizing influence of the wing is most pronounced. At the points labeled B, the whirl frequency  $\omega$  coincides with the wing bending frequency  $\omega_h$  so that whirl motions of the propeller-nacelle system tend to drive the wing at a resonant amplitude. It is suggested in reference 23 that the wing may be considered analogous to a tuned damper which absorbs greatest energy when the system frequency is close to the tuned frequency of the damper.

In the third case shown in figure 13(c) the wing vibration mode involves coupled bending and torsion motions. The frequency of the first coupled wing mode  $\omega_1$  is approximately the same as the uncoupled bending frequency  $\omega_h$  discussed previously, but the mode shape indicates strong coupling between the bending and twisting motions  $h$  and  $\alpha$ . The stability boundary for this condition illustrates an exception to the generally observed trend that wing flexibility stabilizes whirl flutter. It should be noted that the maximum stiffness  $S_\theta$  required occurs in the vicinity of point C where the wing fundamental coupled frequency  $\omega_1$  and the nacelle yaw frequency  $\omega_\psi$  are the same. Since

the wing mode involves pitching of the propeller, point C may be regarded as a coincidence of "pitch" and yaw frequencies for the flexible wing just as point A was for the rigid wing. In both instances the region of instability is extended at these points where the pitch and yaw frequencies coincide.

Thus, a general conclusion of these studies is that a flexible wing has a stabilizing effect on propeller-whirl flutter except possibly in a region where the uncoupled yaw frequency is close to a wing torsion frequency. Beneficial effects of a wing on whirl flutter have also been reported in references 24 and 25.

### Typical Procedures

Analysis of components.- To investigate the flutter characteristics of an aircraft configuration at the preliminary design stage, the following two-phase approach is commonly employed: In the first phase the major components of the aircraft are analyzed individually. For example, on a propeller driven aircraft parametric studies of whirl flutter would be made with the assumption that the propeller-nacelle system is flexibly mounted on a rigid wing structure. These trend studies would include not only the normal mount structure but also various simulated mount failure conditions. Similarly, wing flutter would be studied by assuming that the nacelle-powerplant mass is rigidly attached to the flexible wing.

Then, in the second phase the equations of motion for each component are coupled together and the flutter characteristics of the complete aircraft examined. Usually, a minimum number of parameters are varied in this second phase. Some practical applications of such a flutter analysis procedure may be found in references 25 and 26 for the XC-142A and in reference 9 for the CL-44.

Choice of modes.- The advantage of making flutter trend studies on isolated components as a preliminary to computations for the complete aircraft can be readily appreciated when one considers the large number of modes that are generally necessary to adequately represent the coupled wing-nacelle system. Flutter analyses, such as discussed in reference 9 for the CL-44, serve to illustrate this point. Each of four powerplant packages on this aircraft can be defined in terms of 4 degrees of freedom - pitch and yaw rotations about a set of perpendicular axes, and vertical and horizontal translation along these axes - giving a total of 16 degrees of freedom. Since all four engines rotate in the same sense, there is a cross-coupling effect between the symmetric and the antisymmetric wing modes. It may therefore be necessary to consider an asymmetric system; that is, simultaneously include both symmetric and antisymmetric modes in the flutter analysis. Thus, with 16 nacelle modes combined with possibly 10 or 15 wing modes, the flutter analysis may require up to 30 degrees of freedom. For the XC-142A flutter analysis discussed in reference 25, 27 degrees of freedom were included.

Equations of such large order obviously require high-speed computing equipment for solution. However, even with high-speed digital computers, ill-conditioned equations which may exist result in computational difficulties.

### AEROELASTIC MODELS

Wind-tunnel tests of aeroelastic models are commonly employed to supplement analytical investigations of flutter. A recent example of a wind-tunnel program in which propeller-whirl dynamics were carefully simulated in the flutter model is reported in reference 26.

This investigation involved tests of a 1/10-scale aeroelastic model of the XC-142A VTOL aircraft. Each of four engine-gearbox-propeller systems were dynamically scaled on the model. The propellers, although nonpowered, were shafted together to insure that all turned at the same speed. The remarkable degree of detail achieved in the dynamic simulation of the engine-gearbox system is apparent in figure 14. The gearbox is connected to the engine by a multiredundant strut arrangement on the model in the same manner as it is on the aircraft. The flexibility of each strut as well as the overall flexibility between the engine and the gearbox are accurately scaled in the model. The authors of reference 26 stated that the simulation of this one component represented the most difficult design problem on the model.

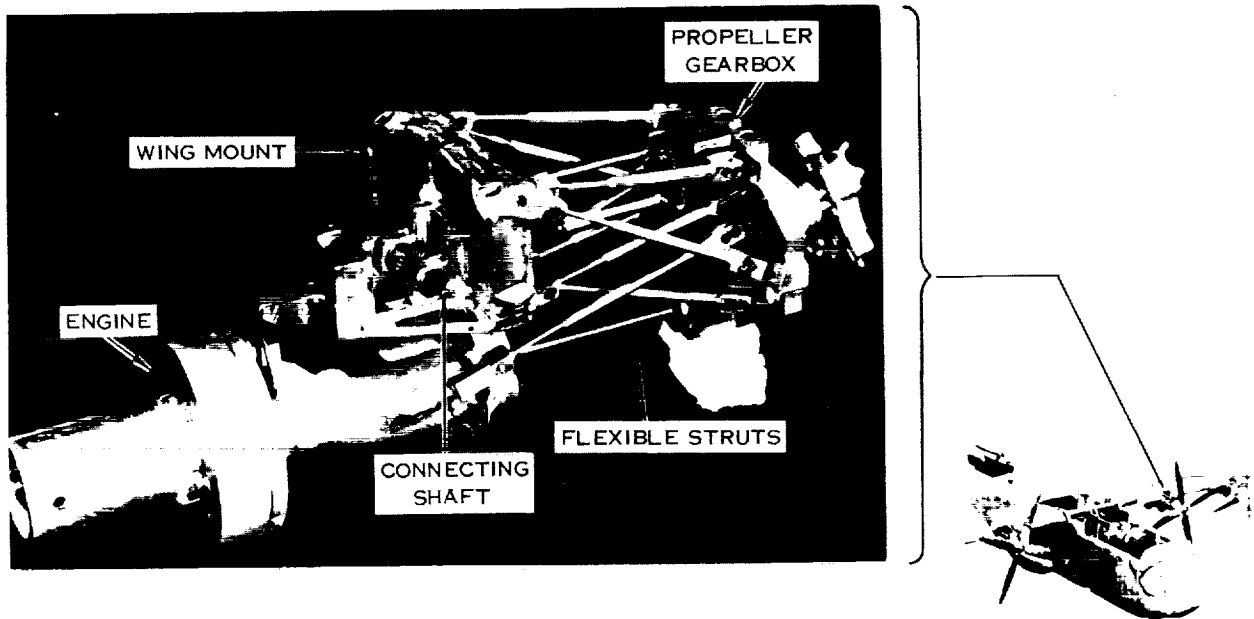


Figure 14.- Engine-gearbox-propeller system used on 1/10-scale dynamic model of XC-142A aircraft (ref. 26).

L-67-1009

A design requirement for the XC-142A was that no flutter occur as a result of failure of any single structural element. (See ref. 7.) Therefore, in the model tests a failure of various strut members was simulated by simply removing the strut in question. The strut failure conditions that were actually simulated on the dynamic model were selected on the basis of analysis. It is interesting to note that in some cases an increase in calculated whirl-flutter speed occurred as a result of a strut failure.

## RESPONSE TO RANDOM ATMOSPHERIC TURBULENCE

Previous sections of this report have dealt with factors that affect the stability of propeller-powerplant systems. A problem of interest related to dynamic loads and fatigue is the response of such systems to gusts and turbulence in the atmosphere. These loads may be significant even though the system is operating well on the stable side of its whirl-flutter boundary.

The gust response problem for a flexibly mounted propeller-powerplant system is briefly considered in reference 14 and a method of analysis suggested. Figure 15, taken

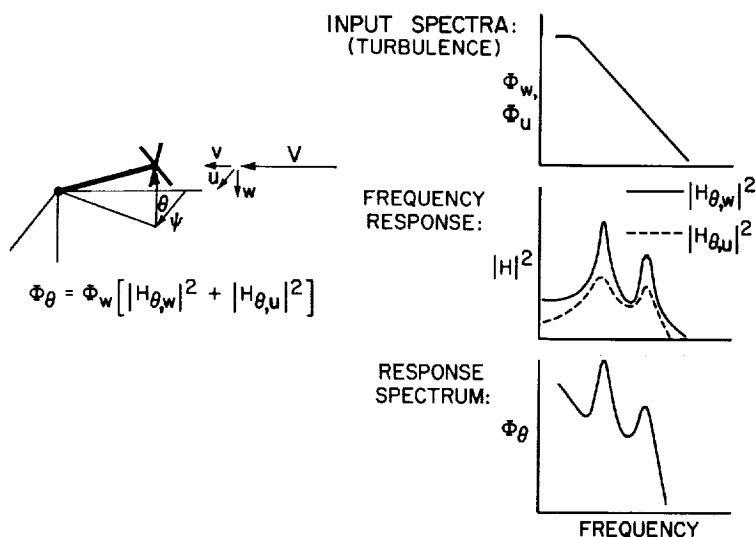


Figure 15.- Response of propeller-nacelle system to random turbulence (ref. 14).

from reference 14, shows the free-stream velocity represented components  $u(t)$ ,  $v(t)$ , and  $w(t)$ . These time-dependent velocities produce unsteady forces and moments on the propeller which in turn cause pitch and yaw deflections  $\theta(t)$  and  $\psi(t)$  of the flexibly mounted system. If turbulence is considered to be a stationary random process, a solution can be obtained for the response of the system to multiple random inputs  $u(t)$ ,  $v(t)$ , and  $w(t)$ . The analysis requires specifications of the power spectra and

cross spectra of the inputs, together with a set of frequency-response functions which define the response of the system to sinusoidal variations of the gust velocity components. If the turbulence is assumed to be isotropic, the cross-spectrum terms of the input become zero and the equation for the power spectrum of response of the system, in pitch, for example, can be written

$$\Phi_{\theta} = \Phi_w \left( |H_{\theta,w}|^2 + |H_{\theta,u}|^2 \right)$$

where  $\Phi_w$  is the power spectrum of the u and w components of turbulence and  $H_{\theta,u}$  and  $H_{\theta,w}$  represent the response in pitch to unit-amplitude sinusoidal u and w inputs. The variation of  $\theta$  due to fluctuations of the longitudinal velocity v, that is,  $H_{\theta,v}$ , has been neglected. The derivation of these equations may be found in reference 14.

The way in which typical power spectra and frequency-response functions for a system might vary with frequency is indicated graphically in figure 15. It should be mentioned that the frequency-response function  $H_{\theta,u}$  – that is, the response in a vertical plane due to a lateral gust input – is a measure of the aerodynamic and gyroscopic coupling produced by the propeller. The two peaks in the response spectrum occur at the backward and forward whirl frequencies. Of these, the peak associated with the backward whirl mode is the larger for two reasons: (1) this mode is more lightly damped than the forward mode, and (2) being at a lower frequency the mode experiences a higher level of the input turbulence spectrum.

#### CONCLUDING REMARKS

A survey is made of the state of the art of propeller-whirl flutter – a precession-type instability that can occur on a flexibly mounted aircraft engine-propeller combination. This report reviews the literature relating to this problem from the time it first became of concern on conventional turboprop and V/STOL aircraft.

Included in the survey are a description of the basic mechanism of whirl flutter, a summary of generalized trend studies on idealized systems, the status of methods for predicting propeller aerodynamic coefficients, the effects of flapping hinged blades and twisted flexible blades on whirl flutter, and some approaches for including propeller-whirl modes as a part of the flutter evaluation for complete aircraft. Also, brief consideration is given to the response of flexibly mounted propeller-nacelle systems to random atmospheric turbulence.

Whirl flutter of conventional propeller-nacelle systems is now a reasonably well understood phenomenon and amenable to analysis. For propeller-rotor systems with flapping blades, however, comparison between experiment and theory suggests the need for further refinements in the mathematical model.

Langley Research Center,  
National Aeronautics and Space Administration,  
Langley Station, Hampton, Va., February 7, 1967,  
721-02-00-06-23.

## REFERENCES

1. Taylor, E. S.; and Browne, K. A.: Vibration Isolation of Aircraft Power Plants. J. Aeron. Sci., vol. 6, no. 2, Dec. 1938, pp. 43-49.
2. Abbott, Frank T., Jr.; Kelly, H. Neale; and Hampton, Kenneth D.: Investigation of Propeller—Power-Plant Autoprecession Boundaries for a Dynamic-Aeroelastic Model of a Four-Engine Turboprop Transport Airplane. NASA TN D-1806, 1963.
3. Reed, Wilmer H., III; and Bland, Samuel R.: An Analytical Treatment of Aircraft Propeller Precession Instability. NASA TN D-659, 1961.
4. Houbolt, John C.; and Reed, Wilmer H., III: Propeller-Nacelle Whirl Flutter. J. Aerospace Sci., vol. 29, no. 3, Mar. 1962, pp. 333-346.
5. Sewall, John L.: An Analytical Trend Study of Propeller Whirl Instability. NASA TN D-996, 1962.
6. Bland, Samuel R.; and Bennett, Robert M.: Wind-Tunnel Measurement of Propeller Whirl-Flutter Speeds and Static-Stability Derivatives and Comparison With Theory. NASA D-1807, 1963.
7. Anon.: Airplane Airworthiness; Transport Categories — Flutter, Deformation, and Vibration Requirements. Civil Air Regulations Amendment 4b-16, FAA, Aug. 31, 1964.
8. Reed, Wilmer H., III: Propeller-Rotor Whirl Flutter: A State-of-the-Art Review. J. Sound Vib., vol. 4, no. 3, Nov. 1966, pp. 526-544.
9. Baker, K. E.; Smith, R.; and Toulson, K. W.: Notes on Propeller Whirl Flutter. Can. Aeron. Space J., vol. 11, no. 8, Oct. 1965, pp. 305-313.
10. Ribner, Herbert S.: Propellers in Yaw. NACA Rept. 820, 1945. (Supersedes NACA ARR 3L09.)
11. Loewy, Robert G.: A Two-Dimensional Approximation to the Unsteady Aerodynamics of Rotary Wings. J. Aeron. Sci., vol. 24, no. 2, Feb. 1957, pp. 81-92, 144.
12. Timman, R.; and Van de Vooren, A. I.: Flutter of a Helicopter Rotor Rotating in its Own Wake. J. Aeron. Sci., vol. 24, no. 9, Sept. 1957, pp. 694-702.
13. Ravera, Robert J.: Effects of Steady State Blade Angle of Attack on Propeller Whirl Flutter. Rept. No. ADR 06-01-63.1, Grumman Aircraft Eng. Corp., July 1963.
14. Reed, Wilmer H., III; and Bennett, Robert M.: Propeller Whirl Flutter Considerations for V/STOL Aircraft. CAL/TRECOM Symposium Proceedings Vol II — Dynamic Load Problems Associated With Helicopters and V/STOL Aircraft, June 1963.

15. De Young, J.: Propeller at High Incidence. *J. Aircraft*, vol. 2, no. 3, May-June 1965, pp. 241-250.
16. Shenkman, Albert M.: Generalized Performance of Conventional Propellers for VTOL-STOL Aircraft. Rept. No. HS-1829 (Contract No. Nonr 2203(00)), United Aircraft Corp., Mar. 31, 1958.
17. Richardson, J. R.; and Naylor, H. F. W.: Whirl Flutter of Propellers With Hinged Blades. Rept. No. 24, Directorate Eng. Res., Defence Board (Can.), Mar. 1962.
18. Hall, W. Earl, Jr.: Prop-Rotor Stability at High Advance Ratios. *J. Am. Helicopter Soc.*, vol. 11, no. 2, Apr. 1966, pp. 11-26.
19. Coleman, Robert P.; and Feingold, Arnold M. (With appendix B by George W. Brooks): Theory of Self-Excited Mechanical Oscillations of Helicopter Rotors With Hinged Blades. NACA Rept. 1351, 1958. (Supersedes NACA TN 3844.)
20. Brooks, George W.: The Mechanical Instability and Forced Response of Rotors on Multiple-Degree-of-Freedom Supports. Ph. D. Thesis, Princeton Univ., 1961.
21. Loewy, R. G.; and Yntema, R. T.: Some Aeroelastic Problems of Tilt-Wing VTOL Aircraft. *J. Am. Helicopter Soc.*, vol. 3, no. 1, Jan. 1958, pp. 35-57.
22. Richardson, J. R.; McKillop, J. A.; Naylor, H. F. W.; and Bandler, P. A.: Whirl Flutter of Propellers With Flexible Twisted Blades. Rept. No. 43, Directorate Eng. Res., Defence Board (Can.), Dec. 1963.
23. Zwaan, R. J.; and Bergh, H.: Propeller-Nacelle Flutter of the Lockheed Electra Aircraft. Rept. F.288, Natl. Lucht- en Ruimtevaartlab. (Amsterdam), Feb. 1962.
24. Bennett, Robert M.; and Bland, Samuel R.: Experimental and Analytical Investigation of Propeller Whirl Flutter of a Power Plant on a Flexible Wing. NASA TN D-2399, 1964.
25. Head, A. L., Jr.: A Review of the Structural Dynamic Characteristics of the XC-142A Aircraft. CAL/TRECOM Symposium Proceedings Vol II - Dynamic Load Problems Associated With Helicopters and V/STOL Aircraft, June 1963.
26. Head, A. L., Jr.; and Smith, W. D.: Dynamic Model Testing of the XC-142A Aircraft. Proceedings of Symposium on Aeroelastic & Dynamic Modeling Technology. RTD-TDR-63-4197, Pt. I, U.S. Air Force, Mar. 1964, pp. 723-762.





.

.

•  
.

